Radio Detection of Colliding Wind Binaries

Paula Benaglia[A,B], *Bärbel Koribalski*[C], *and J.F. Albacete Colombo*[B,D]

[A] Instituto Argentino de Radioastronomía, C.C. 5, Villa Elisa (1894), Argentina

[B] Facultad de Ciencias Astronómicas y Geofísicas, UNLP, Paseo del Bosque S/N, 1900, La Plata, Argentina (email: pbenaglia@fcaglp.unlp.edu.ar)

[C] Australia Telescope National Facility, CSIRO, PO Box 76, Epping, NSW 1710, Australia (email: Baerbel.Koribalski@csiro.au)

[D] Osservatorio Astronomico di Palermo, Piazza del Parlamento 1, I-90134 Palermo (Sicily) Italy (email: facundo@astropa.unipa.it)

Abstract: Four massive, early-type Of stars, three of which are confirmed binaries, have been observed with the Australia Telescope Compact Array at 1.4, 2.4, 4.8 and 8.6 GHz. The earliest star cataloged so far, HD 93129A, was also observed at 17.8 and 24.5 GHz. Here we present an analysis of the spectra as well as the structure of the stellar systems. All four spectra show clear evidence of non-thermal emission, indicative of a binary system with a colliding wind region. We discuss the magnetic field of the emitting region at HD 93129A, and make predictions on the radiation at high energies. Archive X-ray observations towards the target sources are also investigated and interpreted in the light of the non-thermal emission detected.

Keywords: stars: early-type — stars: individual (CD-47 4551, HD 93129A, HD 124314, HD 150136) — stars: mass loss — stars: winds, outflows — radio continuum: stars

1 Introduction

Through supersonic winds massive, early-type stars (OB to Wolf-Rayet) emit particles, as well as their radiation into the circumstellar medium. Spectroscopic measurements show that stellar wind velocities reach thousands of km s^{-1}. The fact that these velocities are larger than the stellar escape velocity proves that important stellar mass loss takes place, especially during and after the end of the main sequence life phase. Mass loss affects the evolution of the star.

The plasma forming the wind produces a thermal excess in flux density from the infrared to the radio range, detectable -and detected- by telescopes with high sensitivity and angular resolution (see the comprehensive observational work by Bieging, Abbott, & Churchwell 1989, for example). However, there are numerous stars that show evidence for non-thermal (NT) emission, revealing the presence of relativistic electrons tangled in the stellar magnetic fields. Local instabilities (e.g. Lucy & White 1980) or magnetic confinement (Jardine et al. 2001) can give rise to particle acceleration in single winds. In a stellar system composed of two stars with interacting winds, relativistic particles are expected to be produced in the region where both winds interact (Eichler & Usov 1993).

In general, early-type stars are X-ray emitters, with a characteristic thermal spectrum, X-ray temperatures of ≥ 1 keV, and X-ray luminosities of about $10^{-7} L_{\rm bol}$ (Berghöfer et al. 1997). In colliding wind binaries, the shock-heated gas at the colliding wind region (CWR) will bring about an enhancement of X-ray emission, which can be considered as a signature of the existence of winds interacting. However, the thermal and/or non-thermal origin of the X-ray radiation strictly depends on the physical parameters and configuration of the stellar system. In close binary systems, the CWR is embedded in the wind acceleration zone: the shocks are less energetic - compared to those in wide systems - and there is thermal radiation mostly at soft X-rays. On the contrary, wide binaries can have strongly colliding winds that produce thermal emission above 3 keV, and are capable of forming the FeK_α 6.7 keV emission line, as well as non-thermal emission from inverse Compton (IC) scattering.

From an observational point of view, the existence of non-thermal X-ray emission does not imply the existence of non-thermal radio emission, because the radio emission forms deep inside the wind where it would be strongly absorbed. However, the inverse situation would be interesting to discuss.

As searches for early-type companions to early-type stars advance, there is diminishing evidence for single stars with non-thermal radio emission. An example is 9 Sgr, an O4 V((f+)), often used to test radio emission models of NT emission from single stars, and very recently re-discovered as a binary with an early-type companion (Rauw et al. 2005). Another rare object is HD 168112, for which radio and X-ray observations show strong evidence of a binary system, while optical observations have been unable to discover a companion (Blomme et al. 2005; De Becker et al. 2004; Rauw et al. 2005).

In a few cases, the CWR has been identified through radio interferometric observations (e.g. WR 146, Dougherty et al. 1996; WR 147, Moran et al. 1989; Cyg

OB2 No. 5, Contreras et al. 1997; WR 140, Dougherty et al. 2005). For WR 146 and WR 147, theoretical calculations of the spatial and spectral distribution of the radio emission were tested against radio data (Dougherty et al. 2003; O'Connor et al. 2005), yielding a good agreement.

For single early-type stars, theoreticians find some difficulties in reproducing the slow decrease in emissivity inside the wind, with the distance to the star, although the latest models involve layered synchrotron emitting regions and the relevant cooling mechanisms (van Loo 2005).

As part of a survey of radio emission from massive, early-type stars, we have performed continuum observations of the brightest, nearest and earliest undetected southern OB stars at 8.6 and 4.8 GHz (Benaglia et al. 2001; Benaglia & Koribalski 2004). Four of the observed stars displayed negative spectral indices ($\alpha < 0$) suggesting a significant non-thermal contribution to their radio emission. We use $S_\nu \propto \nu^\alpha$, where S_ν is the flux density at the frequency ν and α is the spectral index. To further study the radio emission from these stars we also observed them at lower frequencies. Here we present 2.4 and 1.4 GHz observations obtained with the Australia Telescope Compact Array (ATCA[1]) for the stars CD-47° 4551, HD 93129A, HD 124314, and HD 150136. Preliminary results have been presented in Benaglia & Koribalski (2005). Based on the presence of non-thermal radio emission, presumably coming from the colliding wind region of a binary star, we looked for other indicators of binarity. We complemented our analysis of the radio results with a study of all archive X-ray observations towards the stars.

The organization of the paper is as follows: Section 2 gathers the relevant stellar information; Section 3 explains the observing technique and reduction strategy. Section 4 briefly sums up the different mechanisms contributing to the emission from the stars in the radio domain. The radio results are given in Section 5. In Section 6 we analyze the available X-ray data towards the target fields. We discuss the scenario for each object in Section 7, and Section 8 closes with our conclusions.

2 Selected stars

The stars were selected from the targets already observed at 3 and 6 cm (8.64 and 4.8 GHz, Benaglia et al. 2001; Benaglia & Koribalski 2004) that showed a non-thermal contribution to the emission. In order to investigate where the radio emission is coming from, it is fundamental to know the binary status of the stars, and the structure of the systems.

The parameters adopted for the present target stars are listed in Tables 1 and 2. The equatorial coordinates were taken as quoted in the GOS Catalogue (Maíz-Apellániz et al. 2004). The references for the spectral types and wind terminal velocities are given in Table 1. The distances to CD-47° 4551 and HD 124314 are spectro-photometric ones, derived from the apparent magnitude and color index $(B-V)$ quoted as in Benaglia et al. (2001), intrinsic color indices from Wegner (1994) and absolute magnitudes from Martins, Schaerer, & Hillier (2005). The mean molecular weight of the ions (μ) was assumed 1.5 for the earliest types, and 1.3 for the later ones. For the HD 93129A system, the mass loss rate ($\dot{M}$) was taken from Repolust, Puls, & Herrero (2004). The $\dot{M}$ values for the rest of the stars were computed by means of the mass-loss rate recipe given by Vink, de Koter, & Lamers (2000) (astro.ic.ac.uk/jvink). The effective temperatures ($T_{\rm eff}$), stellar masses (M_*), and stellar luminosities (L_*) are from the calibration tables of Martins, Schaerer, & Hillier (2005), obtained with observational $T_{\rm eff}$ scales.

CD-47° 4551, also known as CPD-47° 2963, is the least studied object of the group. Walborn (1982) cataloged it as an O4 III(f). Its binary status is still unknown. Photometric measurements done at CASLEO (San Juan, Argentina), show the absence of another early-type, massive visual companion (P. Ostrov 2001, private communication). Spectroscopic optical observations are currently under way to clarify this issue.

Benaglia et al. (2001) detected CD-47° 4551 with ATCA observing simultaneously at 3 and 6 cm over 160 min. The measured flux densities were $S_{3\rm cm} = 1.77 \pm 0.05$ mJy, and $S_{6\rm cm} = 2.98 \pm 0.05$ mJy. The corresponding spectral index is $\alpha = -0.89 \pm 0.06$.

HD 93129A. This is one of the earliest O star cataloged so far, as O2 If* (Walborn et al. 2002). It belongs to the cluster Trumpler 14, in the Carina region, at 2.5 kpc (Walborn 1995). By means of HST observations Nelan et al. (2004) found the star has an OB companion, 55 mas away (or $\sim$ 140 AU at 2.5 kpc). The companion is assumed coeval and of the same spectral type of various other OB stars nearby (O3.5 V). Recent values of stellar luminosity, mass, effective temperature for the system were derived by Repolust, Puls, & Herrero (2004) in their models taking into account line-blocking/blanketing effects.

At 2.6" (6500 AU at 2.5 kpc) from HD 93129A is the O3.5 V star HD 93129B. A hard X-ray source coincident with the position of the stars was detected by Chandra (Evans et al. 2003, 2004).

The Tr 14 field was observed with the ATCA at 3 and 6 cm (Benaglia & Koribalski 2004), and HD 93129A was the only detection. The measured flux densities were $S_{3\rm cm} = 2.0 \pm 0.2$ mJy, and $S_{6\rm cm} = 4.1 \pm 0.4$ mJy ($\alpha = -1.2 \pm 0.3$).

HD 124314. This target has been classified as an O6 V(n)((f)) by Walborn (1973). Feast, Thackeray, & Wesselink (1954) proposed it as a possible spectroscopic binary (SB1?), and it has a visual companion 2.7" away (about 2700 AU at 1 kpc). This star appears as the main ionising agent of the HII region RCW 85 (Yamaguchi et al. 1999). It has counterparts at other wavelengths: X-rays, the ROSAT source 1RXS J141500.1-614231; IR, the IRAS source 14111-6127, and it is superposed to the probability contours

[1]The Australia Telescope is funded by the Commonwealth of Australia for operation as a National Facility managed by CSIRO.

Table 1: Target sources

Name	RA,Dec (J2000) (hms, dms)	Sp. Type	d (kpc)	$\log(\dot{M})$	v_∞ (km s^{-1})	Status
CD-47° 4551	08 57 54.620 −47 44 15.73	O4 III(f)[a]	1.3[b]	−5.38	[3000][c]	?
HD 93129A	10 43 57.462 −59 32 51.27	O2 If*[d]	2.5[e]	−4.58	3200[f]	Binary[g]
HD 124314	14 15 01.605 −61 42 24.39	O6 V(n)((f))[h]	1.0[b]	−6.15	2500[i]	Binary[d]
HD 150136	16 41 20.415 −48 45 46.64	O3.5 If*[j]	1.3[k]	−5.24	3160[i]	Multiple[j]

[a]Walborn 1982, [b]see text, [c]interpolated from Prinja et al. 1990, [d]Walborn et al. 2002, [e]Walborn 1995, [f]Taresch et al. 1997, [g] Nelan et al. 2004, [h]Walborn 1973, [i]Howarth et al. 1997, [j]Niemela & Gamen 2005, [k]Herbst & Havlen 1977.

of the gamma-ray source 3EG J1410-6147. The study of de Wit et al. (2004) confirms it is a field star.

The star was observed in three opportunities with ATCA at 3 and 6 cm, with flux density variations (see Benaglia et al. 2001, and Table 3).

Table 2: Adopted parameters

Name	$T_{\rm eff}$ (K)	$\log(L_*)$ (L$_\odot$)	M_* (M$_\odot$)	μ
CD-47° 4551	42422[a]	5.85[a]	47[a]	1.5
HD 93129A	42500[b]	6.17[b]	95[b]	1.5
HD 124314	38867[a]	5.32[a]	31[a]	1.3
HD 150136				
"A"	41300[a]	5.96[a]	62[a]	1.5
"B"	38867[a]	5.32[a]	31[a]	1.3

[a]Martins et al. 2005, [b]Repolust et al. 2004.

HD 150136. This star is a member of the open cluster NGC 6193, in the Ara OB1 association, at a distance of 1.3 kpc (Herbst & Havlen 1977). It is the brightest star of a multiple system, with the closest visual component 1.6 arcsec apart, called MIO 8 AB (see Mason et al. 1998, and references therein). The second brightest star in the group is HD 150135, at about 10 arcsec. Very recently, an optical study by Niemela & Gamen (2005), allowed them to re-classify HD 150136 as an O3.5 If* (HD 150136A), to confirm a second close O6 V companion (HD 150136B) with a period of 2.7 days, and suggest a third close OB type component. With these data available a picture of the system can be sketched. For a circular orbit of HD 150136A/B, the separation would be about 40 R$_\odot$ at 1.3 kpc. The visual companion MIO 8AB ($V = 9$) would be separated 0.01 pc (or 2.1×10^3 AU) from HD 150136AB. Both the visual companion spectral type, derived from photometric considerations (later than B3 V), and the large distance from it to HD 150136AB conspire against the existence of a CWR between HD 150136AB and MIO 8AB. We will assume that, if existing, a CWR is located between HD 150136 A & B.

The stellar system is proposed as the ionising source of the HII region RCW 108 (Yamaguchi et al. 1999).

ATCA 3 and 6 cm observations towards the system revealed one non-thermal source of $\sim 2''$ size (at maximum angular resolution) superposed to HD 150136, and a thermal source on HD 150135. The flux densities measured were $S_{\rm 3cm} = 0.28 \pm 0.03$ mJy, $S_{\rm 6cm} = 0.1 \pm 0.04$ mJy for HD 150135, and $S_{\rm 3cm} = 2.61 \pm 0.03$ mJy, $S_{\rm 6cm} = 5.57 \pm 0.03$ mJy for HD 150136.

The cluster NGC 6193 was observed with Chandra (Skinner et al. 2005), and the results are commented in Sect. 6.

3 ATCA observations and data reduction

Radio continuum observations of the four stars listed in Table 1 were obtained with the Australia Telescope Compact Array at 1.4 and 2.4 GHz. The star HD 93129A was also observed at 17.8 & 24.5 GHz.

3.1 Observations at 1.4 and 2.4 GHz

The observations towards the stars CD-47° 4551, HD 93129A, HD 124314, and HD 150136 were carried out in December 2003, in the 6A configuration, simultaneously at 1.384 GHz (20 cm), and 2.368 GHz (13 cm). The total bandwidth used at each frequency was 128 MHz. The average time on source was ∼1 h, except for HD 93129A, which was observed for 6 h. The stars were observed during intervals of 10 to 15 minutes, interleaved with short observations of closeby phase calibrators. The LST ranges spanned were 11 h for HD 93129A, 8 h for CD-47° 4551 and HD 124314, and 6 h for HD 150136. The calibrator source PKS 1934-638 was used to set the flux density scale, with flux densities of 14.94 Jy at 1.384 GHz, and 11.59 Jy at 2.368 GHz.

The data were reduced and analyzed with the MIRIAD package. The calibrated visibilities were Fourier-transformed using "robust"-weighting, which provided the best signal-to-noise ratio combined with sidelobe supression. The shortest baselines were excluded to avoid confussion of diffuse, extended emission.

3.2 Observations at 17.8 & 24.5 GHz

HD 93129A was recently found to be a wide binary formed by two O-type stars (Nelan et al. 2004). Its unique spectral type (O2 If*), and its radio detection at 4.8 and 8.64 GHz as a non-thermal source (Benaglia & Koribalski 2004) make it a very interesting stellar system. In order to get a radio spectrum from 1 to 25 GHz, 12 mm observations were taken in May 2004, at 17.8 and 24.5 GHz (0.17 and 0.12 cm, respectively). Adverse weather conditions reduced the effective observing LST range time to ~ 4 h. We alternately observed the frequency pairs of 17.728/17.856 GHz, and 24.428/24.556 GHz with 128 MHz bandwidth each, to maximize the spectral range, sensitivity, and *uv*-coverage. The target scans were 6 min long, inserted between shorter phase calibrator scans. The absolute flux density was calibrated against Mars and PKS B0607–15.

4 Emission mechanisms

The optically thick wind of a radio star emits thermal radiation by means of the Bremsstrahlung mechanism (Wright & Barlow 1975). At radio frequencies, the thermal flux density, $S_\nu^{\rm T}$, is related to the stellar mass loss rate by:

$$\dot{M} = 5.32 \times 10^{-4}\, \frac{(S_\nu^{\rm T})^{3/4}\, d^{3/2}\, v_\infty\, \mu}{Z\,\sqrt{\psi\, g_\nu\, \nu}} \quad {\rm M_\odot yr^{-1}}\ . \quad (1)$$

Here ψ is the mean number of electrons per ion, Z is the rms ionic charge, and g_ν is the free-free Gaunt factor. In principle, the mass loss rate of an early-type star can be derived in a straightforward manner, by measuring the thermal radio flux density.

However, since the earliest observations of these stars, evidence of a spectral index reaching lower values than the thermal regime arose (Bieging, Abbott, & Churchwell 1989). Emission characterized by such index is explained advocating the presence of energetic electrons embedded in the magnetic fields present in the winds, that are involved in synchrotron emission. The total flux density will have a thermal ($S\nu^{\rm T} \propto \nu_{\rm T}^{\alpha}$, with $\alpha_{\rm T} = 0.6 - 0.8$) and a non-thermal ($S^{\rm NT} \propto \nu^{\alpha_{\rm NT}}$) contribution. It is widely accepted that the relativistic electrons are accelerated by first-order Fermi mechanism in diffusive shocks (Bell 1978), and follow a power-law distribution of the form $N_e(\gamma) \propto \gamma^{-p}$, where $p = 2\alpha_{\rm NT}+1$, and γ is the electron Lorentz factor. The shocks can be present not only in single winds (White 1985), but in the case of a binary system with interacting winds, at the CWR (Eichler & Usov 1993).

As a result of the interaction between the copious UV photons, supplied by the OB star, and the relativistic electrons, high energy emission by IC scattering (Chen & White 1994) is also generated. The IC photon index Γ ($N_{\rm ph}(E) \propto E^{-\Gamma}$) in the Thomson regime is related to p by $p = 2\Gamma + 1$, and hence with $\alpha_{\rm NT}$. If synchrotron and IC losses become important, the electron index is expected to change to $p' = p + 1$ (Longair 1997). The Lorentz factor at which the distribution changes ($\gamma_{\rm b}$) is a function of the average energy density of the photon field, and the average time spent by the particles in the field region (Benaglia & Romero 2003). This last variable depends, in turn, on the size of the non-thermal source and the velocity of the particles, c/k, where k is a normalization parameter.

It is important to consider the effects capable of modifying the radio emission. Part of the synchrotron photons can be absorbed by the wind thermal ions (free-free absorption or FFA). The non-thermal flux can be expressed as $S_\nu^{\rm NT} \propto \nu^{\alpha_{\rm NT}}\, e^{\tau_0 \nu^{-2.1}}$, where τ_0 is the optical depth at which the flux decreases in a factor of $1/e$ (Skinner et al. 1999). The thermal emission can also be absorbed by thermal ions in the so-called internal FFA. Synchrotron self-absorption (SSA) will affect the emission at low frequencies as $S(\nu) \propto \nu^{5/2}$. The critical frequency $\nu_{\rm ssa}$ where this mechanism acts can be expressed as (Williams 1963):

$$\nu_{\rm ssa} \approx 2.145 \left(\frac{S_{\nu_{\rm ssa}}}{\theta^2}\right)^{2/5} B^{1/5}\ {\rm MHz}, \qquad (2)$$

where θ, in arcsec, is the angle subtended by the emitting region, B is the magnetic field at the emitting region in Gauss, and S is the non-thermal flux without absorption, in mJy. The Razin-Tsytovitch effect (RTe) will be important for frequencies below $\nu_{\rm RT} = 20\, n_{\rm e}\, B^{-1}$ Hz, where $n_{\rm e}$ is the electron density at the emitting region (Pachlolczyk 1970).

5 Results

All four stellar systems were detected at both 1.4 and 2.4 GHz, while HD 93129A was also detected at 17.8 and 24.5 GHz (see Figs. 1–5). The detected radio sources are, as expected, unresolved. For CD-47° 4551, HD 124314, and HD 150136 the flux densities and spectral indices measured at 1.4 and 2.4 GHz as well as previous measurements at 4.8 and 8.64 GHz are given in Table 3. The flux densities measured for HD 93129A from 1.4 to 24.5 GHz are given in Table 4. The quoted flux density uncertainties correspond to the measured 1σ rms in the corresponding ATCA image (see Figs. 1–5).

The radio spectra based on the measured flux densities of all four stars show evidence for non-thermal emission suggesting that relativistic electrons are accelerated in shocks, like the ones present in wind-collision regions. The targets were selected because of their non-thermal emission at 3/6 cm, and the trend is confirmed with the 13/20-cm data. The value for the HD 124314 fluxes at 3 and 6 cm (observed three times) were taken as the average of the fluxes detected closer in time, during the year 2000 (see Benaglia & Koribalski 2004 for the details).

While imaging HD 93129A at 17.8 and 24.5 GHz we discovered a new radio source (see Fig. 6). Its position is (RA, Dec)$_{\rm J2000}$ = ($10^{\rm h}43^{\rm m}59.99^{\rm s}$, $-59°33'09.2"$), very close to the star DETWC Tr 14 J104359.9-593309

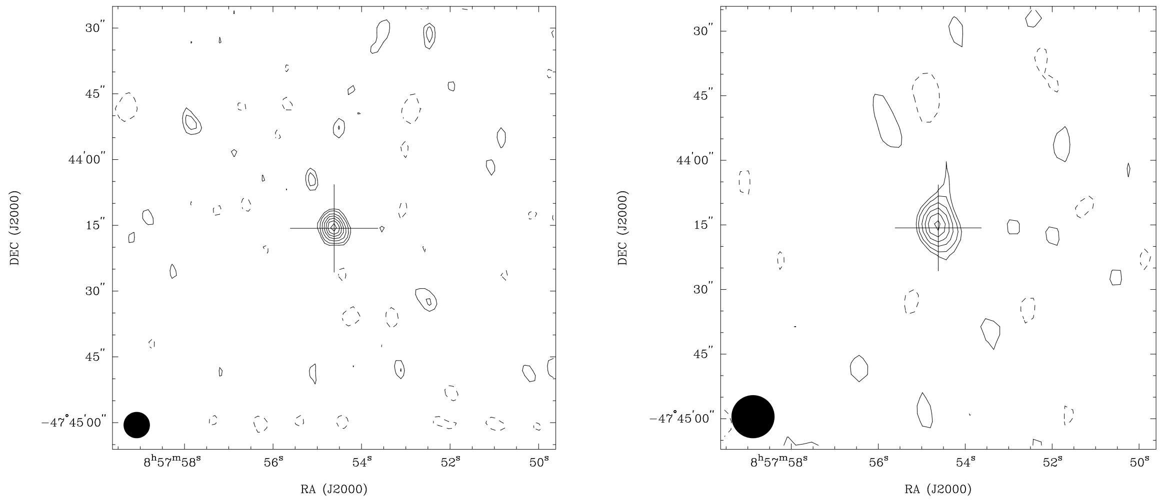

Figure 1: ATCA radio continuum images of CD-47° 4551 at 2.4 GHz (left) and 1.4 GHz (right). In both images the optical position of the star is marked with a cross, and the synthesized beam (6" at 2.4 GHz, and 10" at 1.4 GHz) is displayed in the bottom left corner. The contour levels are –0.7, 0.7 (2σ), 1.0, 1.5, 2.0, 2.5, 3.0, and 3.5 mJy beam^{-1} (left), and –0.8, 0.8 (2σ), 1.2, 1.8, 2.4, 3.0, and 3.6 mJy beam^{-1} (right).

Table 3: Measured flux densities

Star	$t_{\rm int}^{\dagger}$ (min)	$S_{\rm 20cm}$ (mJy)	$S_{\rm 13cm}$ (mJy)	$S_{\rm 6cm}$ (mJy)	$S_{\rm 3cm}$ (mJy)	$\alpha_{13-20{\rm cm}}$	$\alpha_{3-6{\rm cm}}$
CD-47° 4551	61	3.80±0.40	3.82±0.35	2.98±0.05	1.77±0.05	+0.01±0.02	−0.89±0.06
HD 124314	71	2.82±0.40	3.70±0.20	4.14±0.2‡	2.78±0.1‡	+0.50±0.02	−0.64±0.07
HD 150136	43	2.28±0.40	3.05±0.55	5.57±0.03	2.61±0.03	+0.54±0.02	−1.29±0.03

†: at 13/20 cm; ‡: average of fluxes detected in 30/03/2000 and 02/04/2000.

(DeGioia-Eastwood et al. 2001). The measured flux densities are $S_{17.8{\rm GHz}} = 2.2 \pm 0.2$ mJy, and $S_{24.5{\rm GHz}} = 2.6 \pm 0.5$ mJy. The corresponding spectral index is 0.6 ± 0.3, i.e., the expected one for thermal Bremsstrahlung emission from a stellar wind. The visual magnitudes for this star are $V = 13.46$, and $B = 14.76$. If it belongs to the Tr 14 cluster ($d \sim 2.5$ kpc), the spectral type should be between B0 V and B2 V.

Table 4: Flux densities for HD 93129A

Obs. date (dd/mm/yy)	$t_{\rm int}$ (min)	λ (cm)	ν (GHz)	S_{λ} (mJy)
20/12/03	362	20	1.4	9.4±0.9
20/12/03	362	13	2.4	7.8±0.4
28/01/03	298	6	4.8	4.1±0.4
28/01/03	298	3	8.64	2.0±0.2
05/05/04	52	0.17	17.8	1.8±0.15
05/05/04	48	0.12	24.5	1.5±0.35

5.1 Non-thermal emission

The measured fluxes of CD-47° 4551, HD 124314 and HD 150136 presented turnovers along the frequency axis (see Tables 3-4). The flux of HD 93129A diminished with frequencies, but the slighter decrease between 1.4 and 2.4 GHz is indicative that the turnover is beginning to appear towards shorter frequencies. Processes like SSA, RTe, FFA, can contribute to the turnover. Unfortunately, due to the lack of data below 1.4 GHz, and the fact that the turnover is poorly defined, it was not possible to determine which process -and in which manner- shape the spectra at low frequencies.

The strong non-thermal emission found at the stellar spectra is not easy to isolate and characterize, as the processes mentioned above affect it severely. The emitting regions were detected as ATCA point sources, yielding no information on source sizes; additionally, the observational dataset for each star, though covering an important frequency interval, is reduced to 4 points (6 in the case of HD 93129A). Moreover, the flux from a CWR varies with time, depending on the orbit and the relative positions of the two components in a binary system.

However, a rough estimation of the non-thermal spectral index can be done under the following simpli-

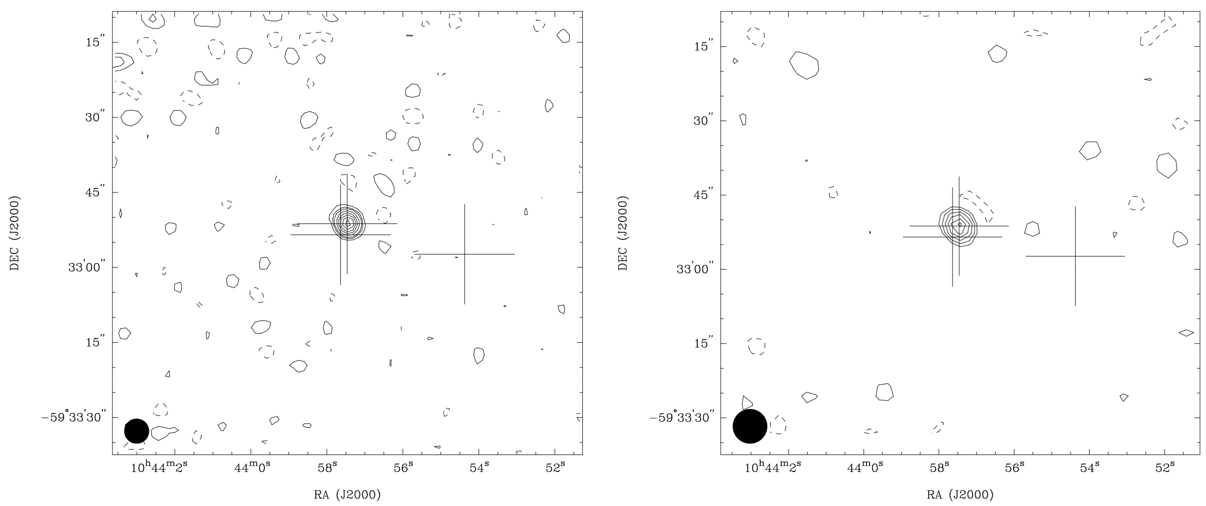

Figure 2: ATCA radio continuum images of HD 93129A at 2.4 GHz (left) and 1.4 GHz (right). In each image the optical positions of the stars HD 93129B, HD 93129A, and HD 93128 (from left to right) are marked with a cross. The synthesized beam (5" at 2.4 GHz, and 7" at 1.4 GHz) is displayed in the bottom left corner. The contour levels are –0.8, 0.8 (2σ), 1.5, 2, 3, ..., and 7 mJy beam^{-1} (left), and –1.8, 1.8 (2σ), 3.0, 4.5, 6.0, 7.5, and 9.0 mJy beam^{-1} (right).

fying assumptions.

We have analyzed the simultaneity of the radio measurements. In the case of HD 93129A, on a first approximation, all the observations can be considered simultaneously taken: the interval between observations was 18 months; the interpretation of very new HST ACS/HRC data combined with the former FGS observations is consistent with a binary of period $\sim$ 50 yr (Maíz-Apellániz et al. 2005). The observations of CD-47° 4551 and HD 124314 covered a time interval of $\sim$3.5 yr. Optical monitoring of radial velocities is needed to test the condition for CD-47° 4551 and HD 124314. On the contrary, the work on HD 150136 by Niemela & Gamen (2005) established that the (O3.5 I + O6 V) form a close pair (period: 2.7 days). That means that each of the radio flux densities presented here should be taken as a mean value, averaged over LST ranges of several h, and precludes any non-thermal flux estimate. Thus, we have assumed that the radio flux densities for CD-47° 4551, HD 93129A, and HD 124314 are quasi-simultaneous, despite the hours interval elapsed during observation.

The search for early-type companions of OB stars has been progressing successfully (Niemela et al. 2006; Rauw et al. 2005), making the existence of single stars with detectable synchrotron radiation look doubtful. Although the binary nature of CD-47° 4551 has to be studied, and the "SB1?" tag of HD 124314 has yet to be confirmed, it seems reasonable to assume that the stars are both (O+OB) binaries and the non-thermal radiation can be produced at a colliding wind region in each system.

If the thermal contribution $S^{\rm T}$ can be subtracted from the observed flux densities (S) at frequencies large enough for which the effects of absorption mechanisms minimize, an un-absorbed non-thermal flux will be obtained. We proceeded to compute $\alpha^{\rm NT}$ between fluxes at 3 and 6 cm, in the way explained below.

We assumed the mass loss rate of each star/system as listed in Table 1, and computed the values for $S^{\rm T}$ from Eq. (1) at 3 cm (8.64 GHz) for $\gamma = Z = 1$. The flux values at 6/3 cm showed also, in general, lower relative errors than the rest, and they were taken simultaneously. For an average thermal spectral index of +0.7, the thermal flux at 6 cm could be derived. With the total and the thermal fluxes at 3 and 6 cm, the estimates of the respective non-thermal flux, and the corresponding spectral index were performed. The resulting values are given in Table 5.

Figure 7 displays, besides the ATCA fluxes, the subtracted thermal contribution, and the residual flux at each observed frequency. It can be appreciated that the values obtained for the thermal contribution in each case were always much smaller that the non-thermal ones: the non-thermal CWR emission seems to dominate over any thermal emission from the individual stellar winds.

Table 5: Estimates of NT indices at 3-6 cm

Star	$S^{\rm T}_{\rm 3cm}$ (mJy)	$S^{\rm NT}_{\rm 3cm}$ (mJy)	$\alpha^{\rm NT}_{3-6\rm cm}$
CD-47° 4551	0.16	1.61	~ -1.0
HD 93129A	0.50	1.50	~ -1.5
HD 124314	0.04	2.74	~ -0.7

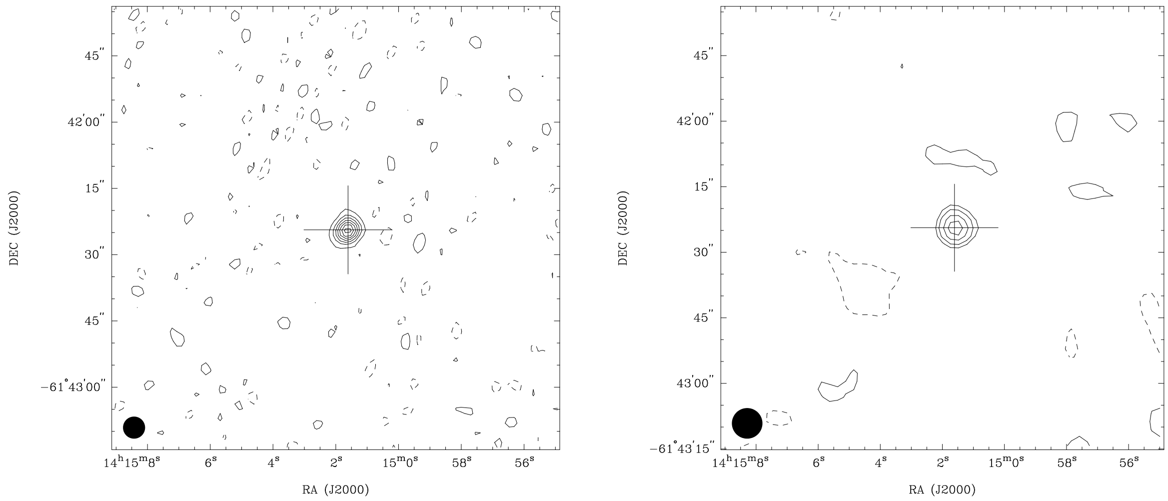

Figure 3: ATCA radio continuum images of HD 124314 at 2.4 GHz (left) and 1.4 GHz (right). In both images the optical position of the star is marked with a cross, and the synthesized beam (5" at 2.4 GHz, and 7" at 1.4 GHz) is displayed in the bottom left corner. The contour levels are –0.4, 0.4 (2σ), 1.0, 1.5, 2.0, 2.5, 3.0, and 3.5 mJy beam^{-1} (left), and –0.8, 0.8 (2σ), 1.2, 1.6, 2.0, and and 2.4 mJy beam^{-1} (right).

6 Stellar X-ray emission

OB stars - either single or multiple - are known X-ray detectable emitters (Berghöfer et al. 1997; Chlebowski & Garmany 1991), with X-ray luminosities $\succ 10^{-7} L_{\rm bol}$. However, some X-ray features are considered as evidence of a colliding wind region, like larger luminosities, or the presence of the FeK$_\alpha$ emission line, produced at wide-binaries collisions events.

Parallely, whereas low-mass flare activity produces a highly correlated behavior between X-ray and radio emission, in OB stars such emission mechanisms remain open to different interpretations.

The four target stars have been detected as non-thermal radio emitters. They are very hot, luminous, and massive. One is cataloged as a binary with another early-type star (HD 93129A), and it was detected at radio waves despite its large distance (2.5 kpc). HD 124314 is also a binary, and presented flux variations up to 40% (Benaglia et al. 2001). HD 150136 belongs to a multiple system with other OB stars. Finally, there is no binary information about the fourth object, CD-47° 4551. We proceeded to investigate on their X-ray emission from literature data, in order to check if they fulfill the $L_{\rm X}/L_{\rm bol}$ ratio for OB stars, if in any case this ratio exceeds the canonical value (indicative of strong shocks at a CWR), and, if spectroscopic data were available, to look for the FeK$_\alpha$ complex.

6.1 X-rays from CD-47° 4551

ROSAT archive data were found on the field of CD-47° 4551. The investigation on stellar X-rays was performed using 4 ROSAT-PSPC X-ray observations towards this star (see Table 6). The angular resolution of these data is about 45 arcsec. The image FOV is 6.32 × 6.32 degrees, and the scale is 15" per px. Our analysis was carried out using the XIMAGE and PIMMS (Portable Interactive Multi-Mission Simulator) software.

We first extracted the photon count rates over a radius of 2', which include more that 90% of the PSF encircled energy. Due to the high pixel scale, the circle encompasses other optical (Digitized Sky Survey: DSS[2]) sources in the field (see Figure 8-a), though the resolution of the X-ray data does not allow to distinguish between emission from nearby stars. However, only two B stars were cataloged over that circle according to the SIMBAD database, enabling us to disregard their X-ray contribution, and conclude that the O4 III star dominates the observed X-ray emission.

According to the different ROSAT energy images (Figure 8-b,c,d), the observed X-ray emission appears quite hard, above 1 keV. We measured count rates in three X-ray bands: a wide band in 0.1-2.4 keV; a soft band (S) in 0.1-0.5 keV; and a hard band (H) between 0.5-2.0 keV. Furthermore, we estimated the hardness ratio as (H-S)/(H+S), yielding an average of 0.91±0.09. This result implies that most (about 70%) of the emitted X-ray energy lies between 1.0 and 2.4 keV (see Table 7). The low signal-to-noise ratio of the observation prevents us from estimating count-rate error values, although we confirm that the average total count rate for CD-47° 4551 is $1.13\pm0.08 \times 10^{-3}$ cts s^{-1}.

It was previously settled that non-thermal radio emission is produced by the synchrotron mechanism, and can be described at 3/6 cm by an index $\alpha_{\rm NT} = -1.0$ (see Sect. 5). The X-ray emission is hard; the scattering processes are more important at several stellar radii, where the UV photon density is larger. It

[2]The Digitized Sky Survey was produced at the Space Telescope Science Institute under US Government grant NAG W-2166.

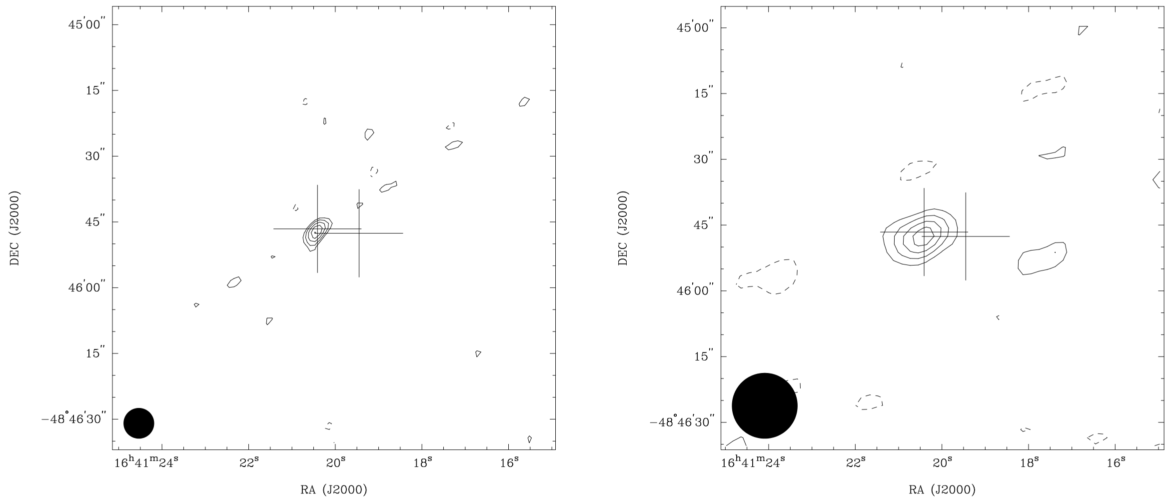

Figure 4: ATCA radio continuum images of HD 150136 at 2.4 GHz (left) and 1.4 GHz (right). In each image the optical positions of the stars HD 150136 (left) and HD 150135 (right), are marked with a cross. The synthesized beam (7" at 2.4 GHz, and 15" at 1.4 GHz) is displayed in the bottom left corner. The contour levels are –1.1, 1.1 (2σ), 1.5, 2.0, 2.5, and 3.0 mJy beam^{-1} (left), and –0.8, 0.8 (2σ), 1.2, 1.6, and 2.0 mJy beam^{-1} (right).

Table 6: Rösat X-ray observations of CD-47° 4551

ROSAT Data	Start Obs. Date	Exposure Time (s)	Offset (deg)	Id. #
rs932518n00	30/10/1990	25642	3.54	1
rs932519n00	11/11/1990	22941	4.04	2
rs932616n00	30/10/1990	29050	4.15	3
rs932617n00	11/06/1990	21783	3.63	4

Note: The Offset refers to the angular distance between the FOV center and the position of CD-47° 4551.

will be expected then that inverse Compton processes are responsible for the observed hard X-ray emission, as well as that absorption processes are related to the outer layers of the stellar wind. We have assumed that X-rays originate in wind layers external enough to be almost un-affected by stellar absorption, enabling us to neglect the wind/X-ray interaction. A strong shock in the O4 III star is originated when the wind reaches velocities close to the terminal velocity, at several stellar radii. At this point, the wind density (and thus the absorption produced by the wind) is very low. We considered that only neutral absorption processes associated with the ISM are affecting the X-rays from this source, and adopt a cold absorption model.

We calculated the total Galactic HI column density using the Web version of the $N_{\rm HI}$-FTOOL software[3], and estimated an interstellar column of neutral hydrogen $N_{\rm HI}$ of 0.92×10^{22} cm^{-2}.

The X-ray count rate can be converted to fluxes using the PIMMS, yielding an un-absorbed flux of 1.35×10^{-13}, 0.024×10^{-13}, and 0.76×10^{-13} erg cm^{-2} s^{-1} for the total, soft and hard bands, respectively.

At a distance of 1.3 kpc, the total X-ray luminosity of CD-47° 4551 is then $L_{\rm X}\sim2.73\times10^{31}$ erg s^{-1}. From the calibration tables of Martins et al. (2005), we adopt a value $\log(L_{\rm bol}/{\rm L}_\odot)$=5.85, and $L_{\rm X}/L_{\rm bol}$ is 1.2×10^{-8}.

6.2 X-rays from HD 93129A

The target HD 93129A is placed at the core of the Trumpler 14 open cluster in the Carina Nebula, one of the most observed regions in X-rays. We found 10 available *XMM-Newton* X-ray observations towards this particular stellar system. Seven of these were centered at the LBV η Carinae star, while the rest are centered at the WR 25 system (WN7+abs). At these pointing directions HD 93129A shows an offset of 11.767" and 10.455", respectively. These differences imply changes in the PSF as well as the encircled energy radii: in the most favorable situation (observations centered at WR 25, see Table 8), the 90% of encircled energy needs an extraction radius of 40". In order to disentangle the contamination from

[3]http://heasarc.gsfc.nasa.gov/cgi-bin/Tools/w3nh/w3nh.pl

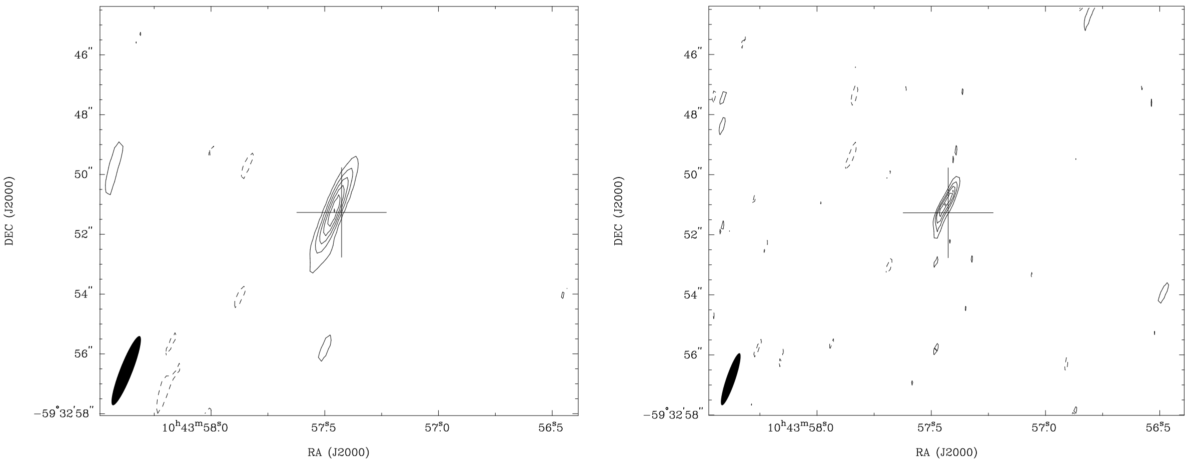

Figure 5: ATCA radio continuum images of HD 93129A at 17.8 GHz (left) and 24.5 GHz (right). In both images the optical position of the star is marked with a cross, and the synthesized beam (2.4" × 0.4" at 17.8 GHz, and 1.8" × 0.3" at 24.5 GHz) is displayed in the bottom left corner. The contour levels are –0.3, 0.3 (2σ), 0.6, 0.9, 1.2, 1.5, and 1.8 mJy beam^{-1} (left), and –0.7, 0.7 (2σ), 1.0, 1.2, and 1.4 mJy beam^{-1} (right).

Table 7: Source count-rates in 10^{-3} cnt s^{-1} and hardness ratio for CD-47° 4551

Id. #	Total [0.1-2.4]	Soft [0.1-0.5]	Hard [0.5-2.4]	H.R. (H-S)/(H+S)
1	1.13	0.04	1.05	0.92
2	1.23	0.03	1.13	0.94
3	0.89	0.07	0.79	0.83
4	1.28	0.05	1.15	0.91
Average	1.13±0.08	0.05±0.02	1.08±0.08	0.91±0.09

nearby sources in the resulting HD 93129A spectrum, we used an extraction radius of 11", in which the fraction of the encircled energy is only about 60%. In doing this, we favored the extraction of an uncontaminated HD93129A spectrum against losing some X-ray photons from the external zone of the PSF (downgrading statistics). The final angular resolution of the image resulted in ~ 6 arcsec, over a FOV of 30 arcmin.

Most massive stars are known to display thermal X-ray spectra with strong and broad emission lines (Kahn et al. 2001; Cohen et al. 2003), contributed by non-thermal emission arising from IC scattering of UV photons due to the presence of a population of relativistic electrons (Pollock 1987; Chen & White 1991; Eichler & Usov 1993). However, HD 93129A seems to display several emission lines from low to high energies (see Figure 9). Such emission lines can only be produced by high-temperature thermal plasma; consequently, the spectral analysis presented here was performed using solely a combination of thin thermal emission models.

Our spectral fits were performed using combined data from all EPIC cameras, in order to improve statistics and discard any instrumental dependence that could be produced by the different responses of the detectors. The spectral model fitted consisted of a combination of absorption and emission models. Two separate absorption columns were used: *i*) one based on the (WABS) atomic cross section (Morrison & McCammon 1983) to account for the action of the circumstellar medium, and *ii*) the second with the ionized absorber model (ABSORI, Done et al. 1992) to include the effect of the stellar wind absorption processes. The first absorption component is due to the neutral material and hydrogen column density, which was calculated and fixed at $N_{\rm H} = 0.52 * E(B-V) \times 10^{22}$ cm^{-2} $= 0.286 \times 10^{22}$ cm^{-2} (Shull & van Steemberg 1985). Here $(B-V) = 0.22$ (Walborn et al. 2002). Table 9 gives the results of the fits. The variable $N_{\rm w}$ stands for the absorption model of ionized wind material, which was left as a free parameter along the whole fitting procedures. Given the high signal-to-noise ratio of the EPIC spectra (below 4 keV), we easily resolve single and blended spectral emission lines from O VIII, Fe XVII (0.825 keV), Mg XI (1.352 keV), Si XIII (1.864 keV), Si XIV (2.006 keV), Si XIII (2.182 keV), S XV (2.460 keV), S XVI (2.622 keV), Ar XVII (3.139 keV) and Ca XX (4.107 keV). Because of the wide range of temperature (3×10^6 to 6.2×10^7 K) needed to form these emission lines, some of them cannot be fitted by the two-temperature model (see Figure 9). Moreover, there seems to be evidence of line excess about 4.8 keV and 6.6 keV. Unfortunately, the poor quality of the data above 4 keV does not allow us to check for the presence of the Fe XXV 6.4+6.7

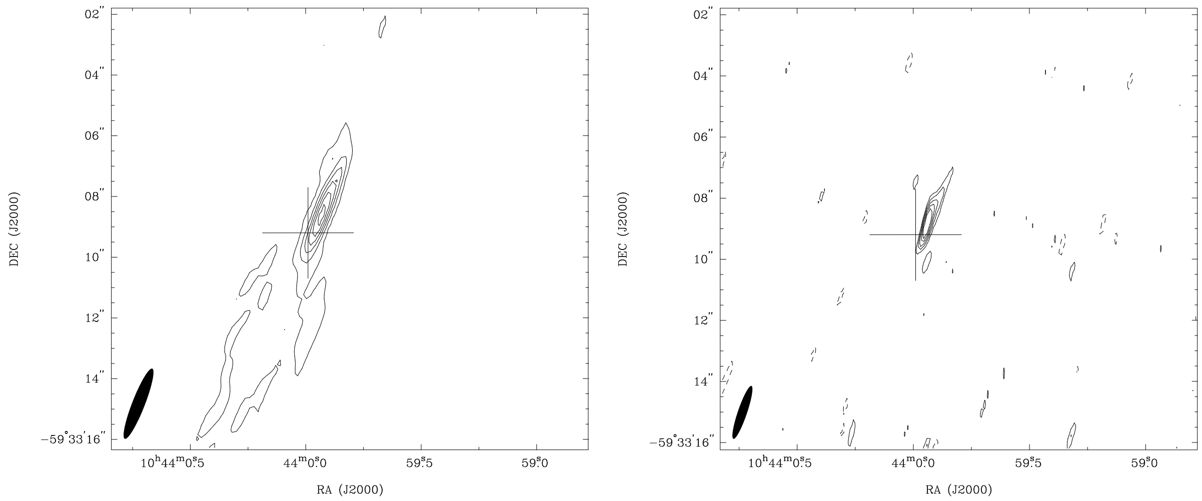

Figure 6: ATCA radio continuum images of the star DETWC Tr 14 J104359.9-593309 (DeGioia-Eastwood et al. 2001), 17.8 GHz (left) and 24.5 GHz (right). In both images the optical position of the star is marked with a cross, and the synthesized beam (2.4" $\times$0.4" at 17.8 GHz, and 1.8" $\times$0.3" at 24.5 GHz) is displayed in the bottom left corner. The contour levels are –0.4, 0.4 (2σ), 0.8, 1.2, 1.6, 2, and 2.4 mJy beam^{-1} (left), and –1, 1 (2σ), 1.4, 1.8, 2.2, and 2.6 mJy beam^{-1} (right).

Table 8: XMM-Newton X-ray observations of HD 93129A

Obs	XMM-Newton	Start Obs.	Exposure	Count rate (10^{-3} cnt s^{-1})		
Id.	Data Set	Date	Time (s)	PN	MOS1	MOS2
1	0112560101	25/06/2001	14000	–	53.8	47.5
2	0112560201	28/06/2001	29000	151.1	53.1	45.0
3	0112560301	30/06/2001	31000	148.2	50.6	48.9

Note: The given values in column 4 are quite approximate because of the slight difference between exposure time of the MOS1, MOS2, and PN observations.

keV line complex that could help us to constrain the thermal and/or non-thermal emission at the hard part of the spectrum. Such detailed study can only be developed using high resolution spectroscospic data, not published at the moment.

Solar abundances are assumed throughout the whole fitting procedure. EPIC MOS and PN fitting results appear very consistent, and our models reveal no significant differences in the quality of the fit. Both procedures are nearly equivalent within the error bars of the models. The goodness of the fit was estimated using the χ^2_ν statistics, and values obtained for all EPIC instruments are quite similar. Adopted parameters were estimated using all EPIC spectra simultaneously.

In the 0.5 – 10.0 keV range, we calculated an observed X-ray flux of 5.66×10^{-13} erg cm^{-2} s^{-1}, while the corrected absorbed X-ray flux is 78.0×10^{-13} erg cm^{-2} s^{-1}. For a source distance of 2.5 kpc, the unabsorbed X-ray luminosity is $L_{\rm X} = 4.51 \times 10^{33}$ erg s^{-1}. According to the spectral type of HD 93129AB, its bolometric luminosity is about 1.20×10^{40} erg s^{-1}, then $L_{\rm X}/{\rm L_{bol}} = 3.75 \times 10^{-7}$. This value agrees with the canonical $L_{\rm X}/L_{\rm bol}$ relationship for O type stars of the region (Albacete Colombo, Méndez, & Morrell 2003).

6.3 X-rays from HD 124314

We found just one X-ray candidate in the HEASARC master compilation of X-ray sources within 0.05° of the HD 124314 position, at (RA, Dec)$_{\rm J2000}$ = ($14^{\rm h}15^{\rm m}00^{\rm s}.934$, $-61°42'19.91"$). This source was detected by the ROSAT All-Sky Survey of Faint Sources Catalog (RASSFSC), and is named 1RXS J141500.1-614231, with a total exposure time of 13472 s. We estimated a total count rate of 1.82×10^{-3}, $0.36 \pm 0.0 \times 10^{-3}$, and 1.45×10^{-3} cts s^{-1} in the total (wide) (0.11-2.4 keV), S (0.2-0.5 keV), and H (0.5-2.4 keV) energy bands, respectively. We also estimated a hardness ratio (H-S)/(H+S) of about 0.60$\pm$0.09. We expect the star emits detectable X-rays; the fact that HD 124314 is a field star, combined with the positional coincidence between the star and the X-ray source lead us to assume that the X-ray source is physically related with the star.

At a distance of 1 kpc (de Wit et al. 2004), we computed a total Galactic H I column density of 1.84×10^{22} cm^{-2}.

With the PIMMS software we calculated an unabsorbed X-ray flux of $2.67{\times}10^{-13}$ erg cm^{-2} s^{-1}. The estimated ratio $\log(L_{\rm bol}/{\rm L_\odot}) = 5.32$ for this star. Then,

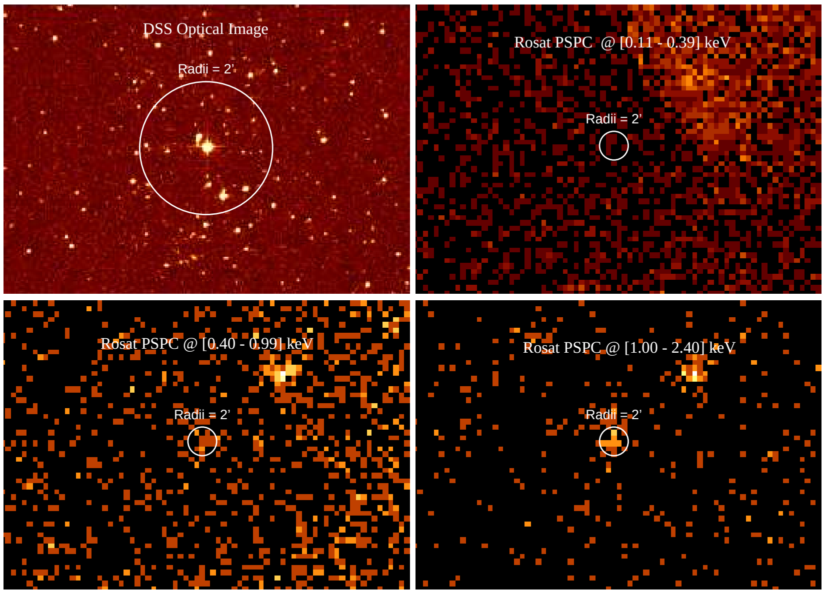

Figure 8: Optical and X-ray observation of the CD-47° 4551 star. **a**: DSS field towards CD-47° 4551. **b-c-d**: ROSAT emission at the bands 0.11 – 0.39, 0.40 – 0.99, and 1.0 – 2.4 keV.

Table 9: Parameters of the EPIC spectra at HD 93129A$^{(1)}$

Obs	$N_{\rm w}$	Mod. 1	Norm. 1	Mod. 2	Norm. 2	Statistic	Flux [0.5-10.0keV]	
Id.	(10^{22} cm^{-2})	kT$_1$ (keV)	10^{-3}	kT$_2$ (keV)	10^{-3}	χ^2_ν/d.o.f	Abs.	Un-abs.
1†	1.08±0.12	0.31±0.03	6.67±0.02	2.18±0.45	0.44±0.01	0.57/119	$6.54^{7.02}_{5.46}$	$112^{132.6}_{90.0}$
2	0.85±0.07	0.30±0.02	4.75±0.01	1.57±0.12	0.49±0.01	0.62/702	$5.79^{6.16}_{5.21}$	$82.5^{94.2}_{60.1}$
3	0.84±0.04	0.29±0.01	4.48±0.08	1.42±0.04	0.55±0.05	0.99/625	$5.66^{5.88}_{5.33}$	$78.0^{83.4}_{66.9}$

(1): Results are given for MOS1, MOS2, and PN combined observations and fitted simultaneously. The cold absorption component is frozen at 0.286×10^{22} cm^{-2}. The normalization parameter (Norm.) of the model is defined as $10^{-14}/(4\pi D^2) \int n_e n_{\rm H} dV$. Flux are in units of 10^{-13} erg cm^{-2} s^{-1}. † The EPIC PN camera was not used due to bad calibrated events in the PN observation. Quoted errors refer to 1σ errors.

$L_{\rm X}/L_{\rm bol}$ is about $0.83{\times}10^{-7}$.

6.4 HD 150136 in X-rays

Berghöfer et al. (1997) identified a ROSAT source of $L_{\rm X}(0.1 - 2.4{\rm keV}) = 1.12 \times 10^{33}$ erg s^{-1}, with HD 150136, though the emission came also from HD 150135. In order to both determine the precise origin of this emission, and study the emission process, Skinner et al. (2005) performed Chandra observations towards the cluster NGC 6193, during 90 ks. They found a soft photon energy distribution from HD 150136, interpreted as indicative of the presence of shocks in the winds.

The results of their 2T model fitting (0.35 ± 0.04, and 1.00 ± 0.07 keV), assuming $N_{\rm HI} = 4 \times 10^{21}$ cm^{-2}, yielded an X-ray flux of 3.3×10^{-12} erg cm^{-2} s^{-1}, and $L_{\rm X} = 2.45 \times 10^{33}$ erg s^{-1} at the (0.5 – 6) keV band, obtaining $L_{\rm X}/L_{\rm bol} = 3.98 \times 10^{-7}$.

The spectrum of HD 150136 presented by Skinner et al. (2005) showed broad lines. They also reported flux variability on timescales of hours, and proposed it can be produced by ocultation effects from a third, and optically unseen, companion (its existence was suggested also by the optical results from Niemela & Gamen 2005).

Table 10 lists the X-ray luminosity and luminosity ratio for the target stars, for comparison.

7 Discussion

7.1 CD-47° 4551 and HD 124314

HD 124314 is listed as a possible spectroscopic binary, and has a visual companion. To proceed with our analysis, the binarity status of this star needs to be confirmed, and the spectral classification of the companion, derived.

CD-47° 4551 is not listed as a binary, and it has no visual companion. Both stars/systems are currently being monitored at optical wavelengths to study their structure.

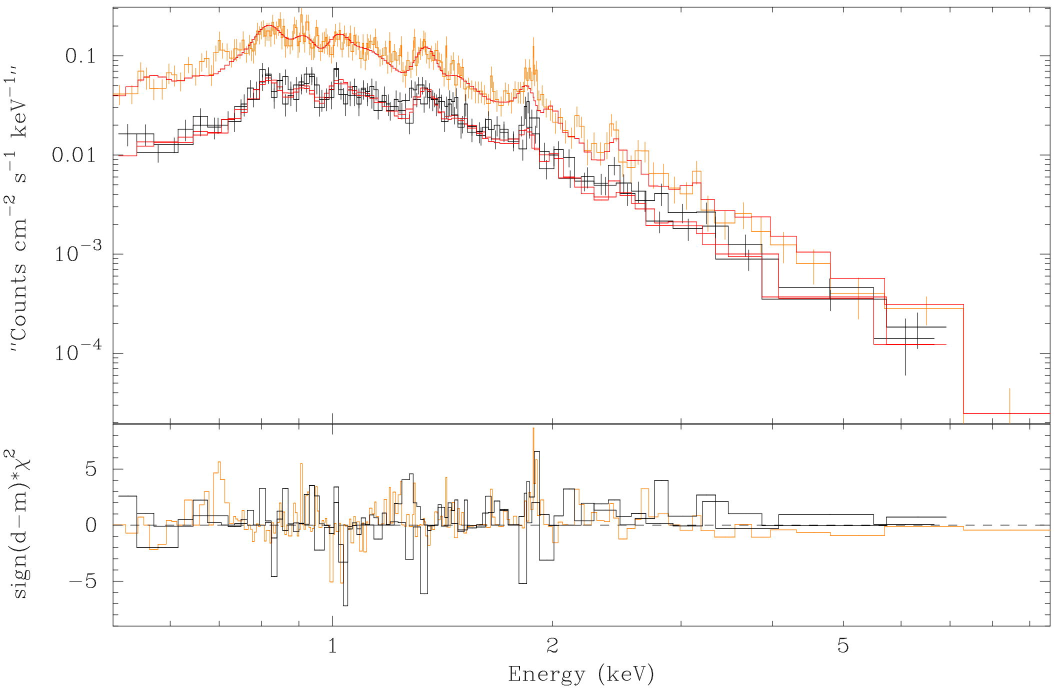

Figure 9: EPIC-PN X-ray spectra of HD 93129A. The PN and MOS spectra were binned to reach a minimum of 4 and 9 counts per channel, respectively. Red line shows the best fit model. Note: The broad observed emission lines (line blending effect) are produced due to the low resolution of the EPIC spectra.

Table 10: X-ray luminosities for the target stars

Star	Energy range (keV)	L_X (erg s^{-1})	L_X/L_{bol} (10^{-7})
CD-47° 4551	0.1 – 2.4	2.73×10^{31}	0.12
HD 93129A	0.5 – 10.	4.51×10^{33}	3.80
HD 124314	0.1 – 2.4	6.70×10^{31}	0.83
HD 150136	0.5 – 6.0	2.45×10^{33}	3.99

The presence of non-thermal radio emission suggests that at least part of the X-ray emission should be non-thermal, too. We found two ROSAT sources: one over CD-47° 4551, and another over HD 124314, which can be generated by relativistic Bremsstrahlung and inverse Compton processes.

The NT spectral index of CD-47° 4551, $\alpha_{3-6\mathrm{cm}} \sim -1$ implies an electron distribution index of $p \sim -1$. For HD 124314, the NT spectral index $\alpha_{\mathrm{NT}} \sim -0.7$, and $p \sim -0.4$.

The difference of the p values with the one corresponding to particle acceleration in a strong adiabatic wind (~ -2) can be found by studying the conditions present at the acceleration region, and depends also on the relevance of the radiative losses. However, the difference can also be taken as an indication that the hypothesis that the observations presented here are quasi-simultaneous has to be revised. Really simultaneous multifrequency observations are needed instead to perform an analysis capable of explaining the radio spectra of these hot stars.

HD 124314 lies inside the location probability contours of the EGRET source 3EG J1410-6147 (Romero, Benaglia, & Torres 1999), one of the few high-energy sources with E > 10 GeV. The counterpart of this EGRET source has been proposed to be the SNR G312.4-0.4 (Torres et al. 2003); nevertheless, a composite origin cannot be ruled out and high energy emission from the stellar system can make a contribution.

7.2 HD 93129A

From the latest optical and radio studies on the stellar system HD 93129A (Nelan et al. 2004; Benaglia & Koribalski 2004) an approximate description of the stellar and orbital parameters can be addressed. The HST data showed a binary separation of 55 mas, or 140 AU, at 2.5 kpc. A wind-momentum ratio $\eta = (\dot{M}_2\, v_{\infty,2})/(\dot{M}_1\, v_{\infty,1}) = 0.14$ is derived, where "1" stands for the primary star, and "2" for the secondary star parameters. The derivation is based on mass-loss rates of 2.3×10^{-5} M$_\odot$ yr^{-1} and 0.3×10^{-5} M$_\odot$ yr^{-1}, and wind velocities of 3200 km s^{-1} and 3000 km s^{-1} for the two stars (Repolust, Puls, & Herrero 2004; Benaglia & Ko-

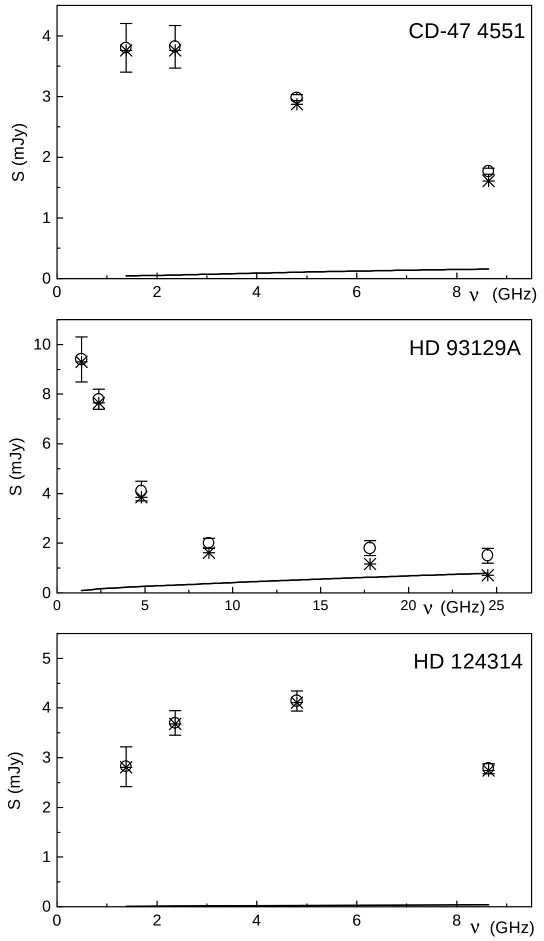

Figure 7: Radio flux densities of the stars CD-47° 4551 (top), HD 93129A (meddle), and HD 124314 (bottom). The open circles mark our measurements, the line indicates the fit for the thermal contribution, and the asterisks, the residuals.

ribalski 2004). These results place the colliding-wind region 15 mas from the companion star, and lead to an estimated CWR size of $\pi r_2 \sim 50$ mas (Eichler & Usov 1993).

The magnitude of the magnetic field as a function of distance, in wide systems, is related to the stellar surface magnetic field B_* by:

$$B(r) = B_* \frac{v_{\rm rot}}{v_\infty} \frac{R_*^2}{r_{\rm A} r} \tag{3}$$

(Eichler & Usov 1993); R_* is the stellar radius, $r_{\rm A}$ the Alfvén radius, and $v_{\rm rot}$ the surface rotation velocity. For early-type stars, $v_{\rm rot} \sim (0.1-0.2)v_\infty$; and $r_{\rm A} \sim (1-3)R_*$.

Only in very few cases a value of the stellar magnetic field could be derived: Donati et al. (2001, 2002) measured B_* for two early-type stars, β Cephei (B1 IV), and θ^1 Ori C (O4-6 V), and obtained the values 360± 30 G, and 1100±100 G, respectively. Theoretical values are about a few hundred G.

Observations at the radio range can give a hint on stellar magnetic fields. When non-thermal radio emission is detected and detached from the thermal flux, an equipartition magnetic field at the CWR can be derived following Miley (1980). The following approximated expression for minimum energy conditions can be used:

$$B_{\rm eq} \approx 100 \left[\frac{1}{\theta^3\, d}\ \frac{1+\chi}{f}\ \frac{S_x^{\rm NT}}{\nu_x^{\alpha\rm NT}}\ \frac{\nu_2^{\alpha'}-\nu_1^{\alpha'}}{\alpha'} \right]^{2/7} \ {\rm mG}. \tag{4}$$

Here θ is the CWR size in mas, $\alpha' = \alpha^{\rm NT} + 0.5$, d is in kpc; χ is the energy ratio between heavy particles and electrons; f is the filling factor of the emitting region; S_x is the flux density in mJy of the region at frequency ν_x, and ν_1 and ν_2 are the upper and lower cut off frequencies presumed for the radio spectrum, these last three parameters expressed in GHz. We have assumed that the energy of particles and electrons is the same and a filling factor of 1.

By means of the ATCA data and a non-radio derived mass loss rate value, we determined a non-thermal spectral index $\alpha^{\rm NT}_{3-6\rm cm} \sim -1.5$ (see Section 5). There is clear evidence from the spectrum that non-thermal emission is present at all wavelengths. For $\theta \sim 50$ mas, an equipartition field at the emitting region of $B_{\rm CWR} \sim 10$ mG is computed, using $x = 8.64$ GHz in Eq. (4), and Table 5[4]. A corresponding (minimum) stellar magnetic field of $B_* \sim 50$ G is derived, by assuming $v_{\rm rot} = 0.2 v_\infty$, $r_{\rm A} = 3R_*$, and $R_* = 20\ {\rm R}_\odot$ (Martins, Schaerer, & Hillier 2005).

For this particular B-field, we can evaluate the frequencies below which the RTe and SSA are relevant. The electron density can be expressed in terms of the mass loss rate of the primary star, as $n_e = \dot{M}_1/(4\pi r_1 v_{\infty 1}\, \mu_1\, m_{\rm H})$, yielding $n_e \sim 6\times10^4$ cm^{-3}, and then $\nu_{\rm RTe} \sim 120$ MHz.

From Eq. (2), $\nu_{\rm ssa} \sim 25$ MHz. Even if the the unabsorbed flux at 1.4 GHz is considered higher than the measured flux (i.e., $5S_{\rm 20cm}$) $\nu_{\rm ssa} \sim 50$ MHz. With the parameters set adopted, if the turnover at 1.4 GHz is ascribed to SSA, the equipartition magnetic field at the colliding wind region would be too high to represent a real scenario.

The non-thermal spectral index $\alpha^{\rm NT}_{3-6\rm cm} = -1.5$, implies an electron distribution with $p = -4$. Explanations of this high value can be found *(i)* if the injected spectrum is sufficiently steep, or *(ii)* if the radio emission is produced by a population of electrons with Lorentz factors above $\gamma_{\rm b}$. An estimate of $\gamma_{\rm b}$ leads to compute the radio frequency at which the spectral index change from $(\alpha^{\rm NT})$ to $(\alpha^{\rm NT}+0.5)$ in $\nu_{\rm b} > 10^6 {\rm k}^{-1}$ GHz. A k value to make $\nu_{\rm b} \sim$ GHz has no physical meaning for relativistic particles.

The maximum Lorentz factor attained by the electrons at the CWR, computed as in Benaglia & Romero

[4] We note that the last value is relevant as an order of magnitude. A different filling factor of, lets say, $f = 0.1$, or a CWR size value halved, would double the value of $B_{\rm CWR}$.

(2003), is $\gamma_{\max} = 1.6 \times 10^5$. This corresponds to a maximum synchrotron frequency of $\nu = 1 \times 10^6$ GHz, and a cutoff energy for the IC photons of $E \sim 5$ GeV.

8 Conclusions

We measured the spectrum of HD 93129A from 1.4 to 24.5 GHz and found the flux decreases with frequency. The negative spectral indices, and the high flux values detected (up to 9.4 mJy) for an O star, are consistent with synchrotron emission from a colliding wind region. An X-ray source coincident in position with the star was found from XMM archive data analysis, and a two temperature spectrum could be fitted which accounts for the many X-ray spectral lines present. The source shows a high $L_{\rm X}/L_{\rm bol}$ ratio of 3.8×10^{-7}, characteristic of OB binaries. The (low) quality of the data above 4 keV prevented us to explore the presence of Fe lines considered as a signature of colliding winds. The hard emission found by Evans et al. (2004) also favors a CWR origin. The intense NT radio emission suggests that the system could be, in principle, detectable with high sensitivity forthcoming gamma ray telescopes.

CD-47° 4551 and HD 124314 are radio non-thermal emitters, and the spectra show a turnover from 1.4 to 8.64 GHz. Their detected fluxes were strongly contaminated with non-thermal emission. Precise (optical) information about the structure of their systems, lacking at the moment, is crucial to reveal the presence of close early-type companions and wind colliding regions, in order to perform a quantitative radio study towards these stars. Both stars are coincident with ROSAT sources, identified here with the stars, and for which we estimated the corresponding luminosity. The $L_{\rm X}/L_{\rm bol}$ ratios obtained for them ($\sim 10^{-8}$) appear low for strong wind collisions: we found no relevant excess when these fluxes are compared with those corresponding to single stars.

HD 150136 is in a multiple system, with at least three early-type stars. Its radio emission also shows important non-thermal contamination, up to 8.64 GHz, though HD 150136 is seen as a point source. To account for the contributions in its radio spectrum, very long-baseline, multifrequency radio observations (separated at most by a few h) are fundamental. The extensive X-ray investigation by Skinner et al. (2005) permits to derive a high $L_{\rm X}/L_{\rm bol}$ ratio of 4×10^{-7}, characteristic of heated gas at a wind collision event.

The picture of these four interesting southern NT OB systems could benefit if at least some of the following studies are pursued: simultaneous radio observations at several frequencies and at higher angular resolution to image and resolve the wind region; optical studies looking for companions, both to discover the structure of the stellar systems and to classify the components; dedicated high angular resolution X-ray observations including spectroscopy, and lastly, high resolution/sensitivity gamma-ray observations.

Acknowledgments

P.B. thanks G.E. Romero for useful discussions, J.B.R., the ATNF staff at Marsfield and Narrabri for constant help, and N.R. Walborn for a critical reading of the manuscript. J.F.A.C. acknowledges support by the Marie Curie Fellowship Contract No. MTKD-CT-2004-002769 of the project "*The Influence of Stellar High Energy Radiation on Planetary Atmospheres*", and the host institution INAF - *Osservatorio Astronomico di Palermo* (OAPA). This research has been supported by the Argentine agency ANPCyT through grant PICT 03 - 13291.

References

Albacete Colombo, J.F., Méndez, M., & Morrel, N.I. 2003, MNRAS, 346, 704

Bell, A.R. 1978, MNRAS, 182, 147

Benaglia, P., Cappa, C.E., & Koribalski, B.S. 2001, A&A, 372, 952

Benaglia, P., & Romero, G. E. 2003, A&A, 399, 1121

Benaglia, P., & Koribalski, B. 2004, A&A, 416, 171

Benaglia, P., & Koribalski, B. 2005, in "Massive Stars in Interacting Binaries", ed. A.F.J. Moffat, & N. St-Louis, in press.

Berghofer, T.W., Schmitt, J.H.M.M., Danner, R., & Cassinelli, J.P. 1997, A&A, 322, 167

Bieging, J.H., Abbott, D.C., & Churchwell, E.B. 1989, ApJ, 340, 518

Blomme, R., van Loo, S., De Becker, M., et al. 2005, A&A, 436, 1033

Chen, W., & White, R.L. 1991, ApJ, 381, L63

Chen, W., & White, R.L. 1994, Ap&SS, 221, 259

Chlebowski, T., & Garmany, C.D. 1991, ApJ, 368, 241

Cohen, D.H., de Messieres, G.E., MacFarlane, J.J. et al. 2003, ApJ, 586, 495

Contreras, M.E., Rodriguez, L.F., Tapia, M., et al. 1997, ApJ, 488, L153

De Becker, M., Rauw, G., Blomme, R., et al. 2004, A&A, 420, 1061

DeGioia-Eastwood, K., Throop, H., Walker, G., & Cudworth, K.M 2001, ApJ, 549, 578

Donati, J.-F., Wade, G.A., Babel, J., et al. 2001, MNRAS, 326, 1265

Donati, J.-F., Babel, J., Harries, T.J., et al. 2002, MNRAS, 333, 55

Done, C., Mulchaey, J.S., Mushotzky, R.F., & Arnaud, K.A. 1992, ApJ, 395, 275

Dougherty, S.M., Williams, P. M., van der Hucht, K. A., et al. 1996, MNRAS, 280, 963

Dougherty, S.M., Pittard, J.M., Kasian, L., et al. 2003, A&A, 409, 217

Dougherty, S.M., Beasley, A.J., Coker, R.F., & Corcoran, M.F. 2005, ApJ, 623, 447

Eichler, D., & Usov, V. 1993, ApJ, 402, 271

Evans, N.R., Seward, F.D., Krauss, M.I, et al. 2003, ApJ, 589, 509

Evans, N.R., Schlegel, E.M., Waldron, W.L., et al. 2004, ApJ, 612, 1065

Feast, M.W., Thackeray, A.D., & Wesselink, A.J. 1954, MmRAS, 67, 51

Herbst, W., & Havlen, R.J. 1977, A&AS, 30, 279

Jardine, M., Collier Cameron, A., Donati, J.-F., & Pointer, G.R. 2001, MNRAS, 324, 201

Kahn, S.M., Leutenegger, M.A., Cottam, J., et al. 2001, A&A, 365, L312

Longair, M. S. 1997, High Energy Astrophysics, Vol. 2, p. 281, Cambridge University Press, Cambridge

van Loo, S. 2005, Ph.D. Thesis, University of Leuven

Lucy, L.B., & White, R.L. 1980, ApJ, 241, 300

Maíz-Apellániz, J., Walborn, N.R., Galué, H.A., & Wei, L.H. 2004, ApJS, 151, 103

Maíz-Apellániz, J., Úbeda, L., Walborn, N.R., & Nelan E.P. 2005, in Resolved Stellar Populations, ASP Conf. Ser., eds. D. Valls-Gabaud, & M. Chávez, in press

Martins, F., Schaerer, D., & Hillier, D.J. 2005, A&A, 436, 1049

Mason, B., Gies, D.R., Hartkopf, W.I., et al. 1998, AJ, 115, 821

Miley, G.K. 1980, Ann. Rev. Astron. Astrophys., 18, 165

Moran, J.P., Davis, R.J., Spencer, R.E., et al. 1989, Nature, 340, 449

Morrison, R., & McCammon, D. 1983, ApJ, 270, 119

Nelan, E.P., Walborn, N.R., Wallace, D.J., et al. 2004, ApJ, 128, 323

Niemela, V.S., & Gamen, R.C. 2005, MNRAS, 356, 974

Niemela, V.S., et al. 2006, in preparation

O'Connor, E.P., Dougherty, S.M., Pittard, J.M, & Williams, P.M. 2005, in Massive Stars and High-Energy Emission in OB Associations, eds. G. Rauw, Y. Nazé, R. Blomme, & E. Gosset, p. 81

Pachlolczyk, A.G. 1970, Radio Astrophysics, Freeman, San Francisco

Pollock, A.M.T. 1987, A&A, 171, 135

Rauw, G., Sana, H., Gosset, E. et al. 2005, in Massive Stars and High-Energy Emission in OB Associations, eds. G. Rauw, Y. Nazé, R. Blomme, & E. Gosset, p. 85

Repolust, T., Puls, J., & Herrero, A. 2004, A&A, 415, 349

Romero, G.E., Benaglia, P., & Torres, D.F. 1999, A&A, 348, 868

Shull, J.M., & van Steenberg, M.E. 1985, ApJ, 294, 599

Skinner, S.L., Itoh, M., Nagase, F., & Zhekov, S.A. 1999, ApJ, 524, 394

Skinner, S.L., Zhekov, S.A., Palla, F., & Barbosa, C.L.D.R. 2005, MNRAS, 361, 191

Torres, D.F., Romero, G.E., Dame, T.M., Combi, J.A., & Butt, Y.M. 2003, PhR, 382, 303

Vink, J.S., de Koter, A., & Lamers, H.J.G.L.M. 2000, A&A, 362, 295

Walborn, N.R. 1973, ApJ, 179, 517

Walborn, N.R. 1982, AJ, 87, 1300

Walborn, N.R. 1995, Rev. Mex. Astron. Astrof., 2, 51

Walborn, N.R., Howarth, I.D., Lennon, D.J., et al. 2002, AJ, 123, 2754

Wegner, W. 1994, MNRAS, 270, 229

White, R.L. 1985, ApJ, 289, 698

Williams, P.J.S. 1963, Nature 200, 56

de Wit, W.J., Testi, L., Palla, F., et al. 2004, A&A, 425, 937

Wright, A.E., & Barlow, M.J. 1975, MNRAS, 170, 41

Yamaguchi, N., Mizuno, N., Moriguchi, Y. et al. 1999, PASJ, 51, 765